Modeling the bioconversion of polysaccharides in a continuous reactor: A case study of the production of oligogalacturonates by Dickeya dadantii

Jacques-Alexandre Sepulchre, Sylvie Reverchon, William Nasser, Jean-Luc Gouzé

Modeling the bioconversion of polysaccharides in a continuous reactor: A case study of the production of oligogalacturonates by *Dickeya dadantii*

Received for publication, June 27, 2018, and in revised form, November 30, 2018 Published, Papers in Press, December 3, 2018, DOI 10.1074/jbc.RA118.004615

Jacques-Alexandre Sepulchre[‡1], **Sylvie Reverchon**[§], **Jean-Luc Gouzé**[¶], **and William Nasser**[§]

From the [‡]*Université Côte d'Azur, Institute of Physics of Nice, UMR7010 CNRS, F-06560 Sophia Antipolis, France, the* [§]*Université Lyon, Université Claude Bernard Lyon 1, INSA-Lyon, CNRS, UMR5240, Microbiologie, Adaptation, Pathogénie, 10 Rue Raphaël Dubois, F-69622 Villeurbanne, France, and the* [¶]*Université Côte d'Azur, Inria, INRA, CNRS, Sorbonne Université, Biocore team, F-06560 Sophia Antipolis, France*

Edited by Chris Whitfield

In the quest for a sustainable economy of the Earth's resources and for renewable sources of energy, a promising avenue is to exploit the vast quantity of polysaccharide molecules contained in green wastes. To that end, the decomposition of pectin appears to be an interesting target because this polymeric carbohydrate is abundant in many fruit pulps and soft vegetables. To quantitatively study this degradation process, here we designed a bioreactor that is continuously fed with de-esterified pectin (PGA). Thanks to the pectate lyases produced by bacteria cultivated in the vessel, the PGA is depolymerized into oligogalacturonates (UGA), which are continuously extracted from the tank. A mathematical model of our system predicted that the conversion efficiency of PGA into UGA increases in a range of coefficients of dilution until reaching an upper limit where the fraction of UGA that is extracted from the bioreactor is maximized. Results from experiments with a continuous reactor hosting a strain of the plant pathogenic bacterium *Dickeya dadantii* and in which the dilution coefficients were varied quantitatively validated the predictions of our model. A further theoretical analysis of the system enabled an *a priori* comparison of the efficiency of eight other pectate lyase–producing microorganisms with that of *D. dadantii*. Our findings suggest that *D. dadantii* is the most efficient microorganism and therefore the best candidate for a practical implementation of our scheme for the bioproduction of UGA from PGA.

The exploitation of biological resources, especially plant waste, is an important issue in economic and ecological terms. For instance, various studies have been initiated during recent decades to generate energy from renewable resources (1). This requires an improvement in knowledge of the degradation of plant complex polymers. The general idea is that these wastes contain a huge quantity of polysaccharides that could be recycled into valuable products, as their components are sugars possessing some economic value. One obstacle, however, to exploiting polysaccharides is their recalcitrance to an effective degradation (2). For instance, although the lignocellulosic resources are the most abundant in biomass wastes, the difficulty of degrading them to elementary components hinders its practical use. Therefore, one strategy is to exploit plants possessing a substantial amount of material more easily degradable than lignin or cellulose, like starch or pectin (2). For example, pectin-rich materials are abundant in some biomass wastes like sugar beet pulp, citrus wastes, or apple pomace (3). In that respect, targeting the transformation of pectin-rich feedstocks offers a perfect resource to improve the efficiency of converting plant cell walls to high-value–added products. Pectin has traditionally found applications in the food industry, mainly as a gelling and thickening agent (4). In recent years, however, there has been an increasing interest in the production and uses of pectin-derived oligosaccharides (POS)[2] and galacturonic acid obtained by depolymerizing the native molecules in small chains of hetero- or homodimers (4–6). Galacturonic acid is used in the food, chemical, and pharmaceutical industries (5, 7, 8), whereas promising applications of the POS are their prebiotic potential and their antitumor activities. For example, POS have been shown to selectively promote the proliferation of beneficial gut bacteria like *Bifidobacteria* spp. and *Lactobacillus* spp., thus improving immunity and metabolism (9). Moreover, recent studies point out the capacity of POS to bind galectin-3 (Gal3), a molecule that is recognized as a key protein enhancing metastatic cancers (*e.g.* in lung, stomach, or colon) (9, 10). In this perspective, POS is currently under study as a potential inhibitor of Gal3, with the great advantage, contrary to anticancer drugs, of not being cytotoxic for normal cells (10). Thus, a wealth of benefits can potentially emerge from bioprocesses able to decompose pectin into oligomers and into monomers. Pectins are complex polysaccharides mainly present in the middle lamella of the plant cell wall. Despite its complexity, the structure of pectin is mainly arranged around backbones formed by α-1,4-linked galacturonic acid residues. Therefore,

This work was initiated in the framework of the project PEPS BMI Pectolyse funded in 2013–2014 by the CNRS, France. The authors declare that they have no conflicts of interest with the contents of this article.
This article contains supporting information.

[1] Supported by a sabbatical stay in the team Biocore of Inria, from January to June 2018. To whom correspondence should be addressed: Université Côte d'Azur, Institute of Physics of Nice, Route des Lucioles 1381, 06560 Sophia Antipolis (Valbonne), France. Tel.: 33-4967340; E-mail: jacques-alexandre.sepulchre@univ-cotedazur.fr.

[2] The abbreviations used are: POS, pectin-derived oligosaccharide(s); Gal3, galectin-3; PGA, polygalacturonic acid(s) or polygalacturonate sodium salt; Pel, pectate lyase; UGA, oligogalacturonates; KDG, 2-keto-3-deoxygluconate.

Table 1

Pectate lyases produced by nine different microorganisms considered in this article characterized by their origin, their GenBank™ accession number, and their classification in the families of polysaccharide lyases, as defined in the Carbohydrate-Active enZYmes Database (14)

The more recent names of organisms have been noted in the first column, but the names used in the review (13) have been included for comparison.

Micro-organism	Characteristic and origin	Pectate Lyase	GenBank accession number	CaZY polysaccharide lyase family
Dickeya dadantii 3937	Plant pathogenic bacterium isolated from Saint Paulia ionantha in France	Pel A Pel B Pel C Pel D Pel E	ADM99550.1 ADN00345.1 ADN00346.1 ADM99552.1 ADM99551.1	PL1 PL1 PL1 PL1 PL1
Amycolata = *Pseudonocardi*	Nonsporulating pectinolytic actinomycetes isolated from a soil sample from Thailand	Pel	AAC38059.1	PL6
Bacillus subtilis	Gram-positive, spore-forming bacterium, commonly found in the rhizosphere and often in association with plant roots	Pel B	CAA52866.1	PL1
Fusarium solani = *Nectria haematococca* mpVI	Plant pathogenic fungi isolated from Pisum sativum (pea).	Pel A	AAA33339.1	PL3
Pseudomonas fluorescens	Bacterium, associated with spoilage of fresh fruits and vegetables	Pel	AAB46399.1	PL6
Azospirillum irakense = *Niveispirillum irakense*	N_2-fixing plant-associated bacterium	Pel A	AAD25394.1	PL10
Bacillus licheniformis	Gram-positive, spore-forming bacterium, commonly found in the rhizosphere and often in association with plant roots	Pel A	CAD56882.1	PL6
Bacillus sp KSM-P15	Gram-positive, spore-forming bacterium, commonly found in the rhizosphere and often in association with plant roots	Pel E Pel H	BAA81752.1 BAA81753.1	PL10 PL9
Fusarium moniliformae = *Fusarium verticillioides*	Pectinolytic fungi isolated from a tropical mangrove community	Pnl	ANC98526.1	PL1

one key target to an effective exploitation of pectic substances is to use efficient enzymes to depolymerize the polygalacturonic acids (PGA). The depolymerases (*i.e.* the class of enzymes acting in the depolymerization of PGA) are divided into three groups according to their mode of action and substrates they prefer: (i) the polygalacturonases (EC 3.2.1.15), (ii) the pectin lyases (EC 4.2.2.10), and (iii) the pectate lyases (Pels, EC 4.2.2.2). Amid the three groups, although these enzymes attack different parts of the pectins, the catalytic efficiency of the pectin lyase is relatively low compared with other depolymerizing enzymes (11). On the other hand, Pels are pectinases forming the most efficient enzymes of these classes of depolymerases (12). In their review, Payasi *et al.* (13) report 32 bacteria able to produce pectate lyases. Among them, nine different microorganisms are considered in this article and are characterized in some detail with reference to the Carbohydrate-Active enZYmes Database (CAZy: http://www.cazy.org)[3] (14) (Table 1). In this table, one of the most effective bacteria is *Dickeya dadantii* (previously called *Erwinia chrysanthemi*). The phyto-pathogenicity of *D. dadantii* is primarily associated with the production of a set of pectinases, mainly several pectate lyases like PelA, PelB, PelC, PelD, PelE, PelZ (15).

Regarding these enzymes, PelB and PelE have the highest specific activities compared with other microbial sources (13). Furthermore, the affinities of the *D. dadantii* Pel enzymes for their polymeric substrates are among the highest compared with other bacteria. Therefore, *D. dadantii* appears *a priori* as one of the most effective bacteria that could be considered for degradation of pectin compounds. The main objective of the present study is to test this hypothesis through a modeling approach and a quantitative analysis of a *continuous stirred-tank reactor* (hereafter referred to as simply a *continuous reactor*). In this system, bacteria are cultivated by continuously feeding a bioreactor with a source of PGA. The latter is enzymatically decomposed into unsaturated oligogalacturonates (UGA) by the action of the pectate lyases secreted by the bacteria. A small fraction of UGA is directly consumed by the microbes for their growth, and the other part of UGA is withdrawn from the tank to be exploited. Based on a previous study (16), we develop a simple mathematical model to predict how the variables of interest of this system will evolve, namely the bacterial biomass, the secreted Pels, and the produced UGA. The aim of our analysis is to design the optimal dilution coefficient to maximize the efficiency of conversion of PGA into UGA. Our model predictions are validated with data obtained from experiments performed in a continuous reactor inoculated with *D. dadantii* in the presence of PGA. On the other hand, our theoretical model enables one to express the conversion efficiency of PGA into UGA as a function of a dimensionless parameter that lumps several biochemical parameters of the system (namely the enzyme–substrate affinity, the V_{max} of the enzyme and its degradation rate, the growth rate and yield of bacteria, and their Monod parameter). Then, combining our analysis with data of the review (13), we are able to compare, at least on the basis of the available parameters, the performance of nine microorganisms with respect to their conversion efficiency of PGA into UGA. The results of our study strengthen the idea that *D. dadantii* should be the best candidate to perform this task.

Under "Results," we report the main analysis done on the mathematical model and compare the predictions with direct measurements taken from growth of *D. dadantii* in a continuous reactor fed with PGA. Also under "Results," we explain how the optimal productivity and conversion efficiency of PGA into UGA can be quantified from the model by considering a key dimensionless parameter characterizing the system. Then under "Discussion," we apply these results to compare the potential efficiencies of PGA-to-UGA conversion of nine different microorganisms able to produce pectate lyases. Finally, we present the experimental procedures and the modeling method for the considered continuous reactor.

Results

Here we present predictions provided by our mathematical model and report experimental results to validate the theoretical analysis. A cartoon representation of that system based on the regulation of *pel* genes is depicted in Fig. 1. The corresponding system of equations (see Equations 6–12) is detailed under "Material and Methods." The main conclusion will be that the bacterium *D. dadantii* could be quite efficient from the perspective of production of UGA oligomers from pectin.

[3] Please note that the JBC is not responsible for the long-term archiving and maintenance of this site or any other third party hosted site.

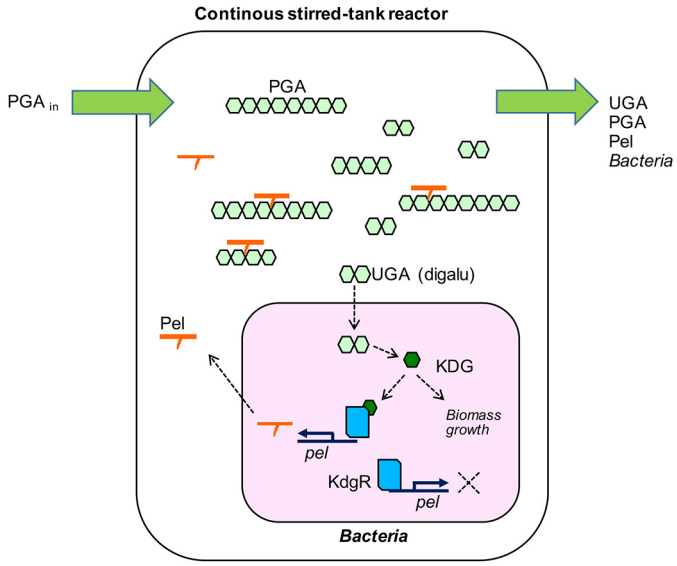

Figure 1. A *schematic representation* of the continuous reactor system. The dynamics can be described qualitatively as follows. The incoming pectin (or PGA_{in}) is decomposed into UGA by the cleavage of Pel enzyme. Extracellular UGA can enter into the bacterium, where it is metabolized into KDG, allowing the increase in the bacterial biomass. On the other hand, KDG acts as an inducer. Indeed, in the absence of UGA, the genes coding for the enzyme Pel are repressed by KdgR, which is the main regulator directly mediating the catabolism of pectin compounds. Once KDG is produced inside the cell, it can bind to KdgR and therefore derepresses the expression of the *pel* genes. It entails a synthesis and export of Pel enzymes in the extracellular medium. Consequently, the expression of the *pel* genes is reinforced while the bacteria grow and its population increases. An equilibrium state results in the continuous reactor when the growth rate of the bacteria is balanced by their outflow from the bioreactor. The objective is to extract from the reactor the greatest possible amount of UGA, which have a high economic value as compared with the PGA.

Analysis of continuous reactor variables and comparison with experiments

The first interesting step to consider for a continuous reactor is the behavior of its stationary regime. Theoretically, the steady states of the reactor are obtained by solving the system of equations (see Equations 6–12), where the time derivatives are replaced by 0. The sought solutions are functions of the dilution coefficient D, defined as the inflow debit feeding the reactor tank, divided by its volume; thus, $D = F_{in}/V$ has a physical dimension of the inverse of time, and $1/D$ can be thought as the residence time of the chemical species in the continuous reactor. In Fig. 2, the stable steady states of system variables have been plotted in the function of D (*solid black lines*). The correspondence between the variable names used in Equations 6–12 and the biochemical names in Fig. 2 is detailed below. In particular, Fig. 2*B* shows the output variable of interest, namely the mass concentration of UGA. In the following, we will call the mass concentration simply the mass.

The mathematical analysis of the system of Equations 6–12 establishes that the non-zero solution branch of UGA is increasing in the function of D. Moreover, it predicts that a bifurcation point is reached for some limit value, $D = D_c$, beyond which the system jumps to the trivial steady state with bacteria no longer in the medium. Indeed, when D is increased, the influx of polymeric substrate is augmented also in the culture vessel. Then the degradation of PGA into UGA increases also, thanks to the Pels produced by the bacteria. At the same time, however, the net growth rate of the bacterial population decreases, due to the loss of the bacteria through the outlet of the culture vessel. This net growth rate becomes negative when $D > D_c$ and thus appears the washout phenomenon of the continuous reactor. For the considered set of parameters, the predicted value of D_c is 0.54 h^{-1}. Experimentally, the washout was already observed for $D = 0.53\ h^{-1}$. Therefore, one can conclude that in practice, $0.4\ h^{-1} < D_c \leq 0.53\ h^{-1}$.

Next, the steady states predicted by the model are experimentally validated. As represented in Fig. 2, experimental data points are obtained by considering the continuous reactor working with five values of the dilution coefficient, namely 0.1, 0.2, 0.3, 0.4, and 0.53. For each of these D values, and at each time point during 14 h, a sample is taken from the medium, and three independent physical variables are recorded, with the following relations between measurements and variables of Equations 6–12. First, the absorbance at 600 nm, denoted as A_{600}, is related to the bacterial fractional volume ρ by the equation, $A_{600} = 10^3\rho$. The second measurement is the absorbance at 230 nm, A_{230}, which is related to mass of UGA by the phenomenological relation, UGA mass $= aA_{230} + b$, as described under "Materials and methods." Finally, the enzymatic activity of the Pels, which is expressed in units of mmol min^{-1}, can be related to the concentration p of Pel by the relation, Act Pel $= k_{cat}p$. These three independent measurements recorded after 14 h enable one to match with the predicted steady-state curves drawn in the *left panels* (*A–C*) of Fig. 2. On the other hand, the same measurements enable us to plot experimental points on the *three right panels* (*D–F*) of Fig. 2. The latter are constructed indirectly from the previous measurements, through three observers of the mass of PGA, the molar concentration of repressor KdgR (variable r in equations), and the molar concentration of the inductor 2-keto-3-deoxygluconate (KDG) (variable i), respectively.

These experimental data are concerned with the (quasi)stationary data collected at the final time $t = 14$ h. Another test to validate the model is to compare the model and experiments during the transient dynamics. This is performed on Fig. 3, showing the transient dynamics of the three directly measured variables, for two fixed values of the dilution coefficient, namely $D = 0.4\ h^{-1}$ (*continuous lines*) and $D = 0.2\ h^{-1}$ (*dashed lines*).

As a whole, the experimental points obtained at steady states and during the transients are well placed with respect to the predicted curves (with some spreading for the enzymatic activities). Regarding the steady states in the function of D, the match is still better when one compares in Fig. 2 the experimental measurements with the numerical simulations of the *pre-equilibrium* curves (*i.e.* the curves obtained at $t = 14$ h) (*dashed curve*). One observes, however, that for $D = 0.53\ h^{-1}$, which is very close to the critical D_c, the washout state is already observed in the experimental data at $t = 14$ h, whereas the model predicts at the same time a state that has a yet larger bacterial density. This means that for $D \sim D_c$, our model is not capturing the right time scale but is describing well the stationary behavior.

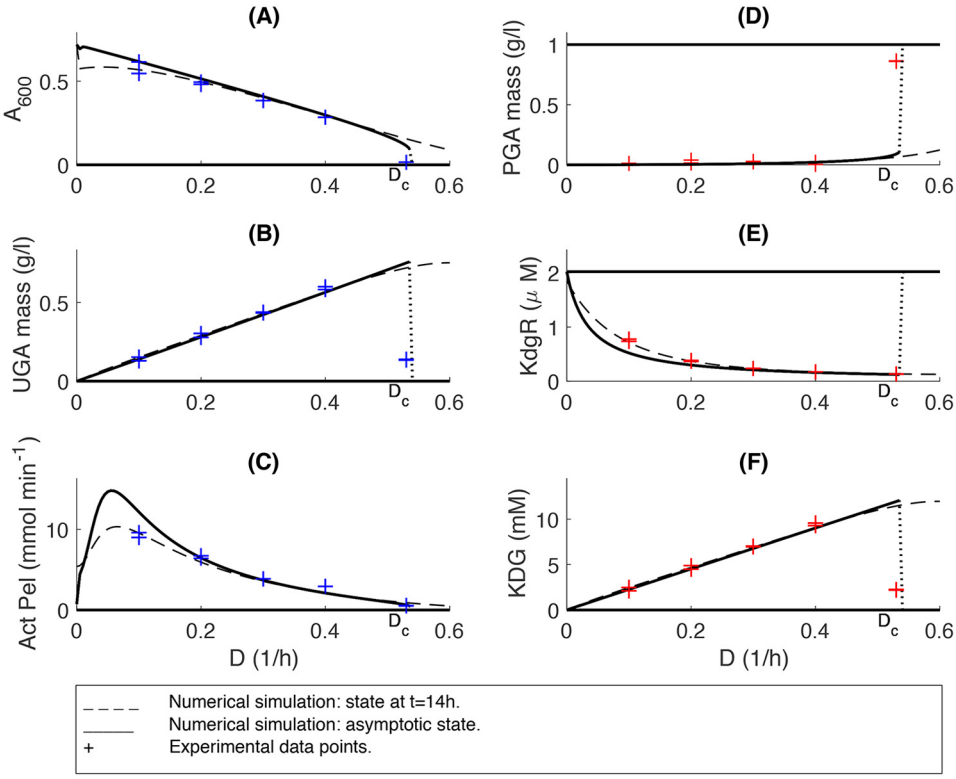

Figure 2. Stationary states of the system variables in a function of the dilution coefficient *D*. The figure shows curves computed by numerical simulations as well as experimental data for five values of *D* (0.1, 0.2, 0.3, 0.4, and 0.53). *Dashed curves*, pre-equilibrium seen for $t = 14$ h. *Continuous curves*, theoretical steady states. The dilution coefficient D_c is a bifurcation point beyond which the non-zero stationary states cease to exist and the washout phenomenon occurs. *A*, optical absorbance at 600 nm is proportional to the bacterial biomass. *B*, UGA mass concentration is extracted from the measurements of the absorbance at 230 nm. *C*, the enzymatic activity is proportional to the concentration of the pectate lyases. *D*, observer of the mass concentration of PGA inside the culture vessel is deduced from the conservation of the mass-equivalent UGA (Equation 13). *E*, observer of the concentration of the repressor KdgR. *F*, observer of the KDG concentration. +, experimental data points.

The use of dimensionless parameters in designing the optimal functioning point

The efficiency of the bioreactor functioning can be evaluated by two quantities: first its *productivity*, which can be defined as the flux of mass of UGA leaving the reactor (expressed in g liter^{-1} h^{-1}). At the stationary state of the system, and regarding the simple mathematical model (Equations 6–12), the flux of mass going out of the reactor can be written as follows,

$$\phi = Du^* M_{\mathrm{UGA}} \qquad \text{(Eq. 1)}$$

where u^* is the steady-state molar concentration of UGA and M_{UGA} is its molar mass. Second, the efficiency of the depolymerization can be quantified by the *conversion efficiency* of the polymeric substrate into oligomers. This dimensionless parameter is defined as follows.

$$\eta = \frac{\text{Outgoing mass of UGA}}{\text{Incoming mass of PGA}} \qquad \text{(Eq. 2)}$$

Thus, η gives the fraction of incoming PGA that is decomposed into UGA and extracted at the reactor outlet. By definition, η is strictly bounded by 1. Indeed, there is always a fraction of incoming PGA that is used for the growth of the bacteria. It can be shown that $\eta = u^*/(ns_{\mathrm{in}})$, where s_{in} is the concentration of the polymer substrate feeding the continuous reactor. Moreover, one can prove that by varying only the dilution coefficient for a given set of system parameters, the *optimal* conversion efficiency, η_{opt}, and the maximal flux, ϕ_{opt}, are attained when the dilution coefficient reaches its limit value $D = D_c$ (17). Finally, the optimal productivity and optimal conversion efficiency are related by the equation, $\phi_{\mathrm{opt}} = \eta_{\mathrm{opt}} D_c \sigma_{\mathrm{in}}$.

There is no closed mathematical expression that formulates η_{opt} or ϕ_{opt} in a function of the system parameters. (These are defined on Table 2.) *A priori* η_{opt} depends on all of the system parameters, and it would be a heavy task to numerically compute the ranges of values that maximize the conversion efficiency by systematically scanning all of the parameter space. In the case of our minimal model, the mathematical analysis of its steady states shows that the best value of η_{opt} can be reached by decreasing as much as possible the following dimensionless parameter,

$$\epsilon = \frac{\gamma \alpha_1 K_m \bar{\mu}}{V_{\max} M_{\mathrm{Pel}} \beta_1 (K_2 + n s_{\mathrm{in}})} \qquad \text{(Eq. 3)}$$

where $V_{\max} M_{\mathrm{Pel}} = k_{\mathrm{cat}}$ (see supporting information). In other words, the analysis shows that $\eta_{\mathrm{opt}}(\epsilon) \to 1$ if $\epsilon \to 0$. To see it intuitively, let us note that when K_2 is larger than ns_{in}, a situation that holds for the considered parameters, then ϵ defined in Equation 3 can be reformulated as follows.

$$\frac{(\gamma \bar{\mu}/K_2)}{(k_{\mathrm{cat}} \beta_1/\alpha_1 K_m)} = \frac{\text{rate of UGA bacteria consumption}}{\text{rate of UGA enzymatic production}} \qquad \text{(Eq. 4)}$$

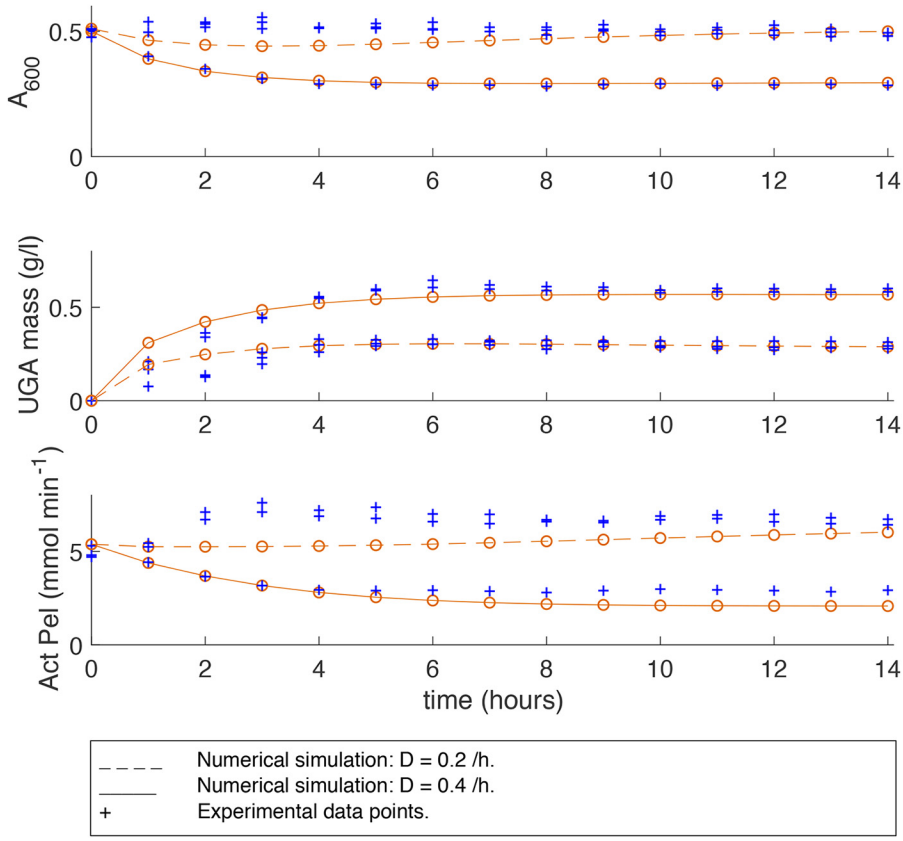

Figure 3. Time evolutions of three variables of interest in the chemostat, for two different values of the dilution coefficient ($D = 0.2\ h^{-1}$ (*dashed lines*) and $D = 0.4\ h^{-1}$ (*continuous lines*)) comparing the experimental measures and the numerical simulations of the theoretical model described by Equations 6–12 with parameters given in Table 2. +, experimental data points.

Table 2
List of parameters

Parameter from literature	Description	value	unit
α_1	degradation of enzymes Pel	$49\ 10^{-3}$	h^{-1}
α_2	degradation of repressor	$35\ 10^{-3}$	h^{-1}
β_2	max. rate of repressor synthesis	$70\ 10^{-9}$	Mh^{-1}
k_{cat}	turnover of enzyme	$4.1\ 10^{6}$	h^{-1}
K_3	affinity KDG-KdgR$_2$	$0.4\ 10^{-3}$	M
K_M	Michaelis Menten const.	$6.8\ 10^{-3}$	M
Parameters identified	**Description**	**value**	**unit**
β_1	max. rate of Pel synthesis	$46\ 10^{-6}$	$M\ h^{-1}$
K_6	dissociation const. of repressor-prom.	10^{-7}	M
γ	yield factor of substrate intake	4	M
k_5	max. rate of KDG phosophorylation	175	h^{-1}
$\bar{\mu}$	max. growth of bacteria	34	h^{-1}
K_2	bact. affinity for digalu	0.14	M
Control parameters	**Description**	**value**	**unit**
σ_{in}	massic external PGA concentration	1	g/l
$\mathcal{M}_{UGA}$	molar mass of dimer UGA	352	g/mol
$s_{in} = \sigma_{in}/(n\mathcal{M}_{UGA})$	external PGA concentration	$1.4\ 10^{-3}$	M
D	Dilution coefficient	0.1; 0.2; 0.3; 0.4; 0.53	h^{-1}

Therefore, the best conversion efficiency of the polymeric substrate will be promoted when ϵ is as small as possible, because in this case, the production of UGA dominates its consumption by the bacteria. The lumped parameter ϵ allows one to compare the optimal conversion efficiency in various systems by ranking their ϵ. An example of an application of this method is reported under "Discussion."

A plot of the graph of η_{opt} in function of $\log(\epsilon)$ is illustrated in Fig. 4. As a matter of fact, our model predicts that η_{opt} possesses a simple linear-logarithmic behavior. This means that in natural scale, the fall of the curve $\eta_{\text{opt}}(\epsilon)$ is quite sharp. In the case of *D. dadantii*, using the parameters of Table 2, one can compute that $\epsilon = 1.7 \times 10^{-3}$, leading to an optimal conversion efficiency of $\eta_{\text{opt}} = 0.75$. Let us note that this conversion efficiency depends on the mass concentration of the incoming PGA from the feeding vessel, which here is fixed to 1 g/liter. For instance, if we double s_{in}, the optimal conversion efficiency diminishes to $\eta_{\text{opt}} = 0.69$. Nevertheless, below, this will be shown to be quite efficient regarding comparative estimates of η_{opt} for other microorganisms (see "Discussion").

Discussion

The first objective of our study was to design a continuous reactor setting to transform PGA into UGA. This is performed thanks to the enzymatic activity of Pels produced by the bacterium *D. dadantii* cultivated in a bioreactor. The goal is to collect at the outlet of the vessel the greatest possible amount of UGA, which possess a greater economic value than the PGA.[4] The main result is that this process can be achieved by increasing the dilution coefficient of the reactor as close as possible of a limit value D_c, but not above, to avoid the washout of the bioreactor.

Let us note that this bioprocess is quite different in a continuous reactor from what would be observed in batch or in fed-batch reactors. To discuss this point quantitatively, Fig. 5 compares the numerical simulations of the mass production of

[4] For instance, the commercial value of purified unsaturated digalacturonate sold by our provider (Sigma) is currently 2,000 times higher than that of PGA.

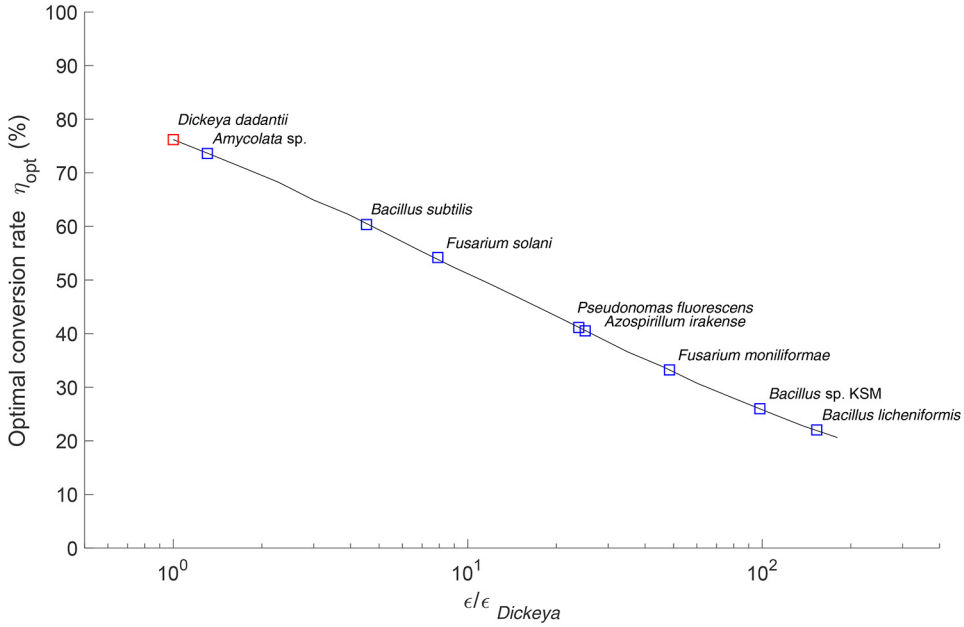

Figure 4. The optimal conversion efficiency η_{opt} of PGA into UGA (*i.e.* the upper limit of produced mass of UGA divided by the incoming mass of PGA) is plotted as a function of the dimensionless parameter ϵ (in linear-logarithmic scale) for the nine microorganisms reported in Table 3. Recall that ϵ is a dimensionless parameter defined in Equation 3 depending on the system parameters, and as such, the smaller it is, the larger is η_{opt}. The *abscissa* is scaled in function of the value of ϵ corresponding to *D. dadantii*. The present graph, comparing the efficiency of nine microorganisms, is performed on the basis of their biochemical parameters listed in Table 3 (K_m, V_{max}, and molar mass of Pel). The other biochemical parameters entering into ϵ being unknown, they are assumed to be equal to the ones of *D. dadantii*. In this approximation, *D. dadantii* appears to be the bacteria possessing the best conversion efficiency of PGA into UGA.

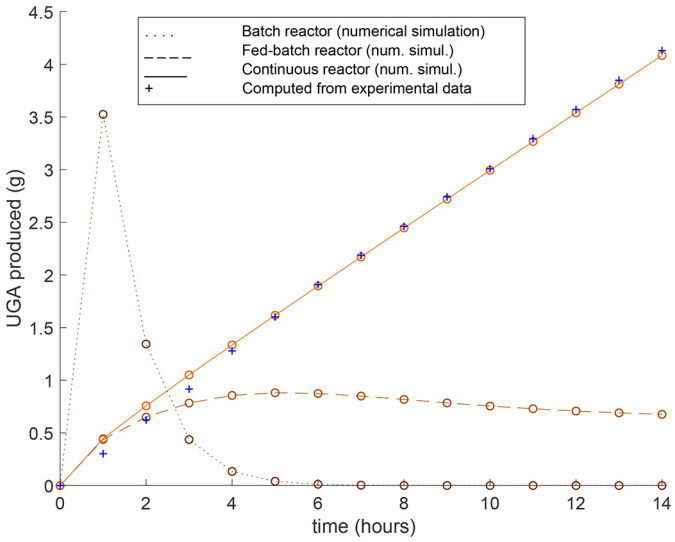

Figure 5. Assuming the same consumption of PGA, comparison of the mass production of UGA predicted by the numerical simulation of our model (Equations 6–12) adapted to three types of biochemical reactors. *Continuous line*, continuous reactor with a constant dilution coefficient D = 0.4 h^{-1} and a reactor volume V_0 = 1.2 liters crossed by a constant volume debit DV_0 = 0.48 liters h^{-1}. After t_f = 14 h, the total consumed volume is $V_f = DV_0\ t_f$ = 6.72 liters. Experimental data of UGA measured from the optical absorbance A_{230} are superposed to the theoretical curve. *Dashed line*, production of UGA in a fed-batch reactor, fed with a constant debit F_{in} = 0.4 liters h^{-1} filling a vessel of initial volume V_0 and reaching a final volume V_f = 6.72 liters after t_f = 14 h. *Dotted line*, production of UGA in a batch reactor of volume V_f = 6.72 liters containing from the beginning the same mass of PGA consumed in the first and second cases (*continuous line* and *dashed line*).

UGA in three different reactor schemes, assuming that the same amount of PGA is consumed in each case. Taking our experiments done with a continuous reactor as the reference, with a dilution coefficient D and a vessel reactor of volume V, the total volume of consumed PGA is $V_f = DVt_f$, where t_f is final time of functioning (*i.e.* 14 h). In batch condition with such a volume, the simulation shows that the PGA is quickly decomposed into UGA, but the latter is next completely metabolized by the bacteria (*cf. dotted line* in Fig. 5, vanishing to 0 after 4–5 h). Interestingly, this numerical computation reveals the existence of a peak of the production of UGA after 1 h, suggesting that an alternative process to produce UGA would be to stop the batch at an appropriate time predicted by our model, in fact before the growth of the bacterial density. On the other hand, a continuously fed reactor creates a permanent dilution effect, which enables the down-regulation of the bacterial density to its minimal value, while the produced UGA is extracted at the outlet of the reactor tank. In the stationary regime of the continuous reactor, the quantity of produced UGA increases linearly in time (*cf. continuous curve* in Fig. 5). Now, in principle, controlling a low bacterial density can also be reached by using a *fed-batch* reactor, where a vessel of volume V_f is gradually filled in by an inflow of debit F_{in}. If the fed batch is performed with a constant volume debit F_{in}, the volume $V(t)$ of the vessel increases so that the dilution rate ($D = F_{in}/V$) decreases (see the legend to Fig. 5 for numerical details). The resulting production of UGA is illustrated by the *dashed line* in Fig. 5. One observes that the initial growth of the production of UGA follows the same behavior as in the continuous reactor, but next the curve stagnates and falls back to smaller values.

Thus, building on a previous mathematical model describing the synthesis of Pel by *D. dadantii* in batch conditions, our minimal system of equations was adapted to the continuous reactor conditions. Keeping the same parameters as previously, the predictions of the new model were observed in a series of experiments, therefore validating the present model. The comparison with experimental data was concerned with the stationary

Table 3
Properties of pectate lyases reported in [13], supplemented by a comparison of η_{opt} and ϕ_{opt} relative to *D. dadantii*

Microorganism (Reference)	Molecular mass	K_m	V_{max}	η_{opt}	ϕ_{opt}
	kDa	*g liter*$^{-1}$	*units/mg protein*	*%*	*g liter*$^{-1}$ *h*$^{-1}$
Dickeya dadantii (average) (15)	41.2	0.26	2,018	76	0.41
Amycolata sp. (23)	31	0.02	158	74	0.38
Bacillus subtilis (24)	42	0.86	1475	60	0.26
Fusarium solani (25)	26	0.13	202	54	0.21
Pseudomonas fluorescens (26)	41	1.28	419	41	0.12
Azospirillum irakense (27)	44.4	0.08	23	40.5	0.12
Fusarium moniliformae (28)	12.1	1.2	655	33	0.08
Bacillus sp. KSM-P15 (29, 30)	20.3	1.87	300	26	0.05
Bacillus licheniformis (31)	33.4	0.56	35	22	0.03

states of the system with various values of the dilution coefficients D, as well as with the dynamical evolution of the system variables for a fixed value of D.

In particular, our study focuses on predicting ϕ_{opt} and η_{opt} (*i.e.* the optimal productivity and conversion efficiency, respectively, of polysaccharides PGA into UGA oligomers). In the case of Pels produced by *D. dadantii*, and considering our parameter set, the theoretical value predicted is $\eta_{opt} = 75\%$. Experimentally, we could reach $\eta_{opt} = 60\%$. However, the purpose was not to optimize this experimental value, as it would require some control setting, as discussed below. The point is that we can retrieve the increasing behavior of η_{exp} in a function of D and confirm that there is a limit value over which the washout phenomenon occurs.

Although the present model is designed with respect to the bacteria *D. dadantii*, it offers some generality for describing the decomposition of polymers by other microorganisms. How can the optimal conversion efficiency of PGA into UGA by *D. dadantii* be matched with other microorganisms able to synthetize pectate lyases? To address this question, one can rely on the study by Payasi *et al.* (13) reviewing some enzymological properties of microbial pectate lyases. On the basis of three main enzymatic parameters (V_{max}, K_m, and molar mass), the other parameters being kept as the ones of *D. dadantii*, the last two columns of Table 3 foresee a tentative comparison of the optimal PGA/UGA conversion efficiencies and productivities between *D. dadantii* and other microorganisms reported previously (13). The corresponding points of η_{opt} are plotted as *squares* in Fig. 4. Certainly, an accurate comparison of the bacterial performances should take into account all of their biochemical parameters. Nevertheless, our method gives a rational ranking of the pectinolytic efficiency of each microorganism reported in Table 3, because the considered parameters in this table are among the most essential in the process of enzymatic degradation. In Fig. 4, the position corresponding to *D. dadantii* maximizes η_{opt}. A relatively closed score is reached by the pectate lyase of *Amycolata*. But the latter microorganism possesses only one type of pectate lyase (*cf.* Table 1), whereas the reference value considered for *D. dadantii* is actually grounded on the *mean* biochemical parameters of its five major pectate lyases, PelA, PelB, PelC, PelD, and PelE, having various performances. Furthermore, *D. dadantii* possesses an arsenal of other genes that can deal with methylated or demethylated pectin. Therefore, *Amycolata* is most likely less efficient than *D. dadantii*, which appears to be the best candidate in view of configuring an actual bioreactor device to transform pectin into UGA.

Let us remark that in this work, the considered substrate is not the standard pectin, but its simplest form corresponding to the PGA. Indeed, the goal of the present study was to achieve as far as possible quantitative results by combining computational modeling and biological experimentations. This would be more complicated with complete pectin because of its various sugars, which involve more metabolic pathways. However, we think that our work has a practical biotechnological utility for the following reason. According to their degree of methoxylation, pectins can be classified as high-methoxyl pectins (50% esterified or higher) or low-methoxyl pectins (less than 50% esterified). Some pectins have a very low degree of methylation. For example, citrus peel pectin from Sigma (catalog no. P9135) has a methoxyl content of ~6.7% and therefore is not so different from PGA used in our experiments. Furthermore, *D. dadantii* produced two pectin methyl esterases (PemA and PemB) and two pectin acetyl esterases (PaeX and PaeY) responsible for pectin de-esterification. Therefore, this bacterium can perform "real-life" pectin biomass conversion.

On the other hand, the analysis of our model shows that in view of working in its optimal regime of UGA production, an issue of the current scheme is that the optimal point of functioning is unstable. Indeed, it corresponds to a bifurcation point of the dynamical system. For $D < D_c$, the steady state of interest coexists with the washout state, whereas just after the point $D = D_c$, the stable equilibrium disappears, and only the washout state is stable. Thus, because the system parameters are not exactly known, and because the parameters can also fluctuate, the optimal state obtained for $D = D_c$ is not robust with respect to parameter uncertainty or external perturbations. A remedy to solve this issue is to consider a control feedback loop on the dilution coefficient D and make it a function of the measurement of the bacterial biomass $\rho(t)$. Actually, in another work, treating a simpler model than Equations 6–12, we have brought the proof of principle of this control method by considering the following control law (17): $D(t) = \delta\rho(t)$, where $\delta > 0$ is a fixed parameter whose value can be chosen to stabilize any stationary point (s^*, u^*, ρ^*) of functioning compatible with the mass conservation law (*cf.* Equation 13).

$$\sigma_{in} = (ns^* + u^* + \gamma\rho^*)\, M_{UGA} \qquad \text{(Eq. 5)}$$

In the current model, preliminary results based on numerical simulations show that this simple control method should also be able to stabilize the optimal point of functioning. Therefore,

a straightforward extension of the present work will be to experimentally implement such a control method.

Conclusion

Although the present model is designed with respect to the bacterium *D. dadantii*, it offers some generality for describing the decomposition of polymers by other microorganisms. The main assumption is that these other organisms express one or several genes coding for pectate lyases and that they can use a part of the decomposed substrate for their growth. As our model prediction for η_{opt} is based on one lumped parameter that combines the main biochemical parameters, this study can be used to compare various organisms, once their parameters are known. Doing so, we claim that the optimal conversion efficiency of *D. dadantii* is quite efficient compared with other bacteria. Therefore, in view of an actual implementation to transform pectin in UGA, the current approach provides experimental data and theoretical analysis to demonstrate the feasibility of the concept and shows that *D. dadantii* is likely to be the best natural microorganism to fulfill this purpose.

Materials and methods

Procedures

Bacterial strain and culture conditions—D. dadantii 3937 (18) was used for all of the experiments described. Cultures were grown at 30 °C in M63 minimal salt medium (19) supplemented with a carbon source: glucose at 0.2% (w/v) and various concentrations of PGA, from 0.05 to 0.2% (w/v). Liquid cultures were grown in a shaking incubator (220 rpm). PGA from Sigma was obtained by de-esterification of citrus peel pectin using fungal pectin methyl esterases. Precultures from single colonies were grown overnight in M63 medium supplemented with glucose. Cells were re-inoculated into 500 ml of M63 medium plus glucose, $CaCl_2$ (0.1 mM), and PGA (0.2% (w/v)), and the resulting medium was grown at 30 °C during 16 h to reach the beginning of the stationary phase. At this stage, all of the PGA added in the growth medium was totally degraded, allowing the induction of Pel production (16). The resulting medium was used for continuous cultures as follows. Briefly, the bioreactor (BiostatR B Plus, Sartorius Stedim) tank containing 900 ml of M63 medium plus $CaCl_2$ (0.1 mM) and PGA (0.01% (w/v)) was supplemented by 100–250 ml of the batch culture to reach a final A_{600} of 0.35–0.5 and Pel activity of 5 units and then start the feeding pump (feeding solution: M63 medium plus $CaCl_2$ (0.1 mM) and PGA (0.1% (w/v)); 1 unit corresponds to 1 μmol of unsaturated product liberated per min and per ml of enzymatic extract). Three aliquots were taken every hour: 1 ml for monitoring the cell growth, 1 ml toluenized immediately for Pel activity quantification, and a 10-ml sample for quantification of the digalacturonate concentration. In the last case, the cells were harvested by a centrifugation of 5 min at 6,000 × *g*, and then 6 ml of the supernatant was taken, adjusted to 1 mM EDTA final concentration, and submitted to an incubation of 20 min at 95 °C to inactivate the Pels contained in the medium. Aliquots of the media taken before inoculation with the bacteria and treated as described above were used as a reference.

Enzyme assays—The assay of pectate lyase was performed on toluenized cell extracts. Pectate lyase activity was determined by monitoring spectrophotometrically the degradation of PGA to unsaturated products that absorb at 230 nm (20). The molar extinction coefficient of unsaturated oligogalacturonates used was 5,200 liters mol^{-1} cm^{-1} (20). Pectate lyase activity is expressed as μmol of unsaturated products liberated per min. The standard assay mixture consisted of 100 mM Tris-HCl (pH 8.5), 0.1 mM $CaCl_2$, and 0.5 g of PGA per liter in a total volume of 1 ml. Bacterial concentration was estimated by measuring turbidity at 600 nm, given that an absorbance at 600 nm (A_{600}) of 1.0 corresponds to 10^9 bacteria/ml with a volume of 0.5 μm^3/cell. Digalacturonate quantification was performed spectrophotometrically at 230 nm.

Model formulation

The theoretical framework used in this study is a mathematical model of the growth of *D. dadantii* in a bioreactor (or chemostat) fed in by PGA. This model is founded on previous work modeling the same bacteria but in batch conditions (16). Here, we extend this first study in two ways. First, the bacterial growth is described by Monod-like kinetics depending explicitly on the substrate, which is a new variable. Previously, the bacterial growth was modeled by a logistic function decoupled from the intake of substrates (16). A second generalization of the initial model is to consider the setting of a continuous bioreactor, which is fed by a source of polymeric substrate with concentration s_{in} and with a coefficient of dilution D. This means that if the culture vessel has a volume V, it is submitted to a constant incoming and outgoing flow DV. Then the time-evolution of the system is described by the following set of equations,

$$\frac{d\rho}{dt} = (\mu(u) - D)\rho \qquad \text{(Eq. 6)}$$

$$\frac{du}{dt} = nk_{cat}p\frac{s}{K_m + s} - \rho\gamma\mu(u) - Du \qquad \text{(Eq. 7)}$$

$$\frac{ds}{dt} = -k_{cat}p\frac{s}{K_m + s} + D(s_{in} - s) \qquad \text{(Eq. 8)}$$

$$\frac{dp}{dt} = \beta_1\left(\frac{\rho}{1-\rho}\right)\frac{K_6}{K_6 + Y_d(r,i)} - (\alpha_1 + D)p \qquad \text{(Eq. 9)}$$

$$\frac{dr}{dt} = \beta_2 - (\alpha_2 + \mu(u))r \qquad \text{(Eq. 10)}$$

$$\frac{di}{dt} = (1-\rho)\gamma\mu(u) - (k_5 + \mu(u))i \qquad \text{(Eq. 11)}$$

where $\mu(u) = \bar{\mu}\frac{u}{(K_2+u)}$ is the growth rate of the bacteria and the following,

$$Y_d = \frac{r/2}{1 + (i/K_3)^2} \qquad \text{(Eq. 12)}$$

is the concentration of the main repressor of the *pel* gene (see below). The state variables of this system are summarized in Table 4, and a detailed justification of each term appearing in the set of Equations 6–12 is provided in the supporting information. The considered variables can be divided in two catego-

Table 4
List of variables

	Description	Unit
Extracellular variables		
$p(t)$	Pel enzyme	mM
$s(t)$	PGA	mM
$u(t)$	UGA	mM
$\rho(t)$	Fractional bacterial volume	
Intracellular variables		
$r(t)$	Repressor KdgR	μM
$i(t)$	Inducer KDG	M

ries: either internal to the bacteria or belonging to the extracellular medium. First, the extracellular variables are as follows. ρ is the fractional bacterial volume (*i.e.* the volume occupied by bacteria divided by the total volume of the vessel). Let us note that here we identify the bacterial biomass with its volume, assuming implicitly that its mass density is constant; next, p is the molar concentration of enzyme pectate lyases in the extracellular vessel; the last extracellular variables, u and s, are the molar concentrations of UGA and PGA, respectively. Here, the cleavage of PGA is described as a single step, PGA $\rightarrow n$ UGA, decomposing a PGA polymer containing n digalacturonates into n dimers. Although we also considered a more detailed model,[5] the experimental data could be fitted equally well with the simplest one, even by considering $n = 2$. Therefore, we decided to stick here with the simpler formalism in the numerical simulations. Second, in what concerns the intracellular variables, they are on one hand r, the molar concentration of KdgR, which is the main repressor of *pel* gene, and on the other hand i, the molar concentration of KDG. This latter molecule is a catabolite product of UGA and plays the role of the *inducer* of the *pel* gene, because it can derepress *pel* expression by binding to the repressor $KdgR_2$ (21).

The model parameters are listed in Table 2, keeping the same notations as the ones used earlier (16). The parameters are divided in three categories. The first category of parameters are taken from the literature, and thus their values are strictly the same as the ones considered in previously (16). The parameters appearing in the second part of Table 2 were all identified in batch experiments, thus independently of the present work, which is concerned with a continuous reactor setting. Some of the parameters in this second part describe the Monod-like growth rate for the biomass, which was not considered in Ref. 16. The third part of Table 2 designates the control parameter of the experiments: the concentration of the feed bottle of the reactor, expressed either in mass concentration (σ_{in}) or in molar concentration (s_{in}). This external control parameter is kept to the fixed value $\sigma_{in} = 1$ g/liter. The only varying control parameter is the dilution coefficient D of the system. All computations concerning the system of ordinary differential Equations 6–12 were performed in Matlab R2017b, using different ordinary differential equation integrators to test the consistency of the numerical results. The stiff integrator ode15s was appropriate most of the time, although non-stiff procedures would work also but with longer integration times.

[5] A detailed model was considered where the fragmentation of PGA is described by taking into account the step-by-step decomposition of the initial polymer into oligomers of all intermediate lengths. A method to derive the kinetic equations for such extended system can be found in Ref. 17.

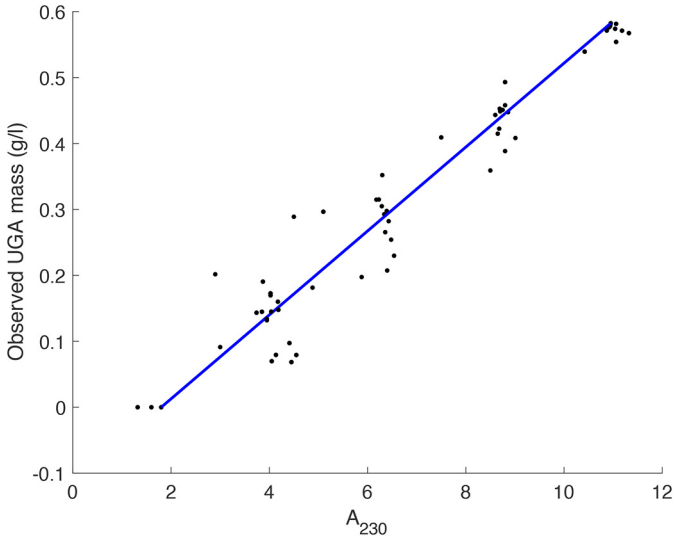

Figure 6. The *straight blue line* shows an affine model (mass concentration of UGA in g/liter = 0.064 A_{230} − 0.11) for the relationship between the absorbance at 230 nm and the mass concentration of the free UGA in the continuous reactor. Each point corresponds to a measure performed at a given time (each hour between 0 and 14 h) and a given dilution coefficient D among 0.1, 0.2, 0.3, and 0.4. This affine transformation is used in Figs. 2 and 3 to plot the mass concentration of UGA measured via the absorbance A_{230}. The abscissa of each point is a measurement of A_{230}, which is matched with the "expected" UGA that is observed via the UGA-equivalent variable w (see "Materials and methods"). A salient feature of this relation is that when the amount of UGA vanishes, the absorbance A_{230} tends to a non-zero value that can be interpreted as a residual absorption of the bulk at 230 nm.

A frequent property of models of bacterial growth is the existence of a global variable describing the mass balance of the substrate and its consumption. Here such variable can be found to be the following,

$$w = (ns + u + \gamma\rho)\, M_{UGA} \qquad \text{(Eq. 13)}$$

where M_{UGA} is the molar mass of UGA dimer. The variable w can be interpreted as a record track of what becomes the mass of PGA entering the continuous reactor, counted in terms of an *equivalent* mass of UGA; the first term, nsM_{UGA}, accounts for the free PGA (with a molar mass n times the one of UGA); the second term of Equation 13, uM_{UGA}, corresponds to the actual UGA produced in the bioreactor, and the last term, $\gamma\rho M_{UGA}$, is the UGA metabolized by the bacteria, with a yield factor γ. Therefore, at equilibrium, when the reactor reaches its stationary state, the mass-equivalent UGA must be equal to the injected mass of PGA, which we introduced above as $\sigma_{in} = 1$ g/liter. This property is useful to make a link between the mass of UGA and the absorbance at 230 nm, A_{230}, which is measured for this purpose (see above). On the other hand, measures of A_{230} on a sample of the culture might be perturbed by the residual absorption of other molecules in the bulk. To simply model the relation between A_{230} and the produced mass of UGA, we first construct an *observer* of UGA (*i.e.* a dynamic system that enables us to indirectly quantify UGA from the measurement of another variable) (22). Indeed, by computing the derivative of w defined in Equation 13, it is readily seen that $dw/dt = D\,(\sigma_{in} -$

w). Thus, the time-evolution of $w(t)$ is given the exponential function, $w(t) = (w(0) - \sigma_{in})\exp(-Dt) + \sigma_{in}$, where $w(0) = ns(0) + \gamma\rho(0)$ can be evaluated from the initial state of the reactor, assuming $u(0) = 0$. Then, from Equation 13, an estimate of the mass of UGA can be deduced from the relation $u_{obs}(t) = w(t) - ns(t) - \gamma\rho(t)$, where $\rho(t)$ is *measured* via the absorbance at 600 nm and $s(t)$ is neglected except at $t = 0$. Indeed, the enzymatic decomposition of PGA appears to be much faster than the time scale over which UGA is measured (*i.e.* hours). The points plotted in Fig. 6 show the *observed* UGA at all considered times of measurement (see below), *versus* direct measures of A_{230} at the corresponding time points. Although the resulting relationship exhibits some stochasticity, it can be approximated by an affine function (*e.g.* UGA mass $= aA_{230} + b$), which is found to be satisfactory to quantify the mass concentration of UGA from direct measurements of A_{230}.

Author contributions—J.-A. S. and J.-L. G. conceptualization; J.-A. S., S. R., and W. N. resources; J.-A. S. software; J.-A. S. formal analysis; J.-A. S. and J.-L. G. supervision; J.-A. S. funding acquisition; J.-A. S. and J.-L. G. validation; J.-A. S., S. R., and W. N. investigation; J.-A. S. visualization; J.-A. S. methodology; J.-A. S. writing-original draft; J.-A. S. project administration; J.-A. S., S. R., J.-L. G., and W. N. writing-review and editing.

Acknowledgment—R. Sarker is acknowledged for some parameter identification of the model during an internship in the summer of 2013.

References

1. Pedrolli, D. B., Monteiro, A. C., Gomes, E., and Carmona, E. C. (2009) Pectin and pectinases: production, characterization and industrial application of microbial pectinolytic enzymes. *Open Biotechnol. J.* **3,** 9–18 CrossRef
2. Xiao, C., and Anderson, C. T. (2013) Roles of pectin in biomass yield and processing for biofuels. *Front. Plant Sci.* **4**, 67 CrossRef Medline
3. Edwards, M. C., and Doran-Peterson, J. (2012) Pectin-rich biomass as feedstock for fuel ethanol production, *Appl. Microbiol. Biotechnol.* **95,** 565–575 CrossRef Medline
4. Gerschenson, L. N. (2017) The production of galacturonic acid enriched fractions and their functionality. *Food Hydrocoll.* **68,** 23–30 CrossRef
5. Combo, A. M. M., Aguedo, M., Goffin, D., Wathelet, B., and Paquot, M. (2012) Enzymatic production of pectic oligosaccharides from polygalacturonic acid with commercial pectinase preparations. *Food Bioproducts Processing* **90,** 588–596 CrossRef
6. Naqash, F., Masoodi, F. A., Rather, S. A., Wani, S. M., and Gani, A. (2017) Emerging concepts in the nutraceutical and functional properties of pectin: a review. *Carbohydr. Polym.* **168,** 227–239 CrossRef Medline
7. Molnár, E., Eszterle, M., Kiss, K., Nemestóthy, N., Fekete, J., and Bélafi-Bakó, K. (2009) Utilization of electrodialysis for galacturonic acid recovery. *Desalination* **241,** 81–85 CrossRef
8. Burana-osot, J, Soonthornchareonnon Chaidedgumjorn, N., Hosoyama, A., and Sand Toida, T. (2010) Determination of galacturonic acid from pomelo pectin in term of galactose by hpaec with fluorescence detection. *Carbohydr. Polym.* **81,** 461–465 CrossRef
9. Zhang, W., Xu, P., and Zhang, H. (2015) Pectin in cancer therapy: a review. *Trends Food Sci. Technol.* **44,** 258–271 CrossRef
10. Kapoor, S., and Dharmesh, S. M. (2017) Pectic oligosaccharide from tomato exhibiting anticancer potential on a gastric cancer cell line: structure-function relationship. *Carbohydr. Polym.* **160,** 52–61 CrossRef Medline
11. Yadav, S., Yadav, P. K., Yadav, D., and Yadav, K. D. S. (2009) Pectin lyase: a review. *Process. Biochem.* **44,** 1–10 CrossRef
12. Dubey, A. K., Yadav, S., Kumar, M., An, G., and Yadav, D. (2016) Molecular biology of microbial pectate lyase: a review. *Br. Biotechnol. J.* **13,** 1–26 CrossRef
13. Payasi, A., Sanwal, R., and Sanwal, G. (2009) Microbial pectate lyases: characterization and enzymological properties. *World J. Microbiol. Biotechnol.* **25,** 1–14 CrossRef
14. Lombard, V., Golaconda Ramulu, H., Drula, E., Coutinho, P. M., and Henrissat, B. (2014) The carbohydrate-active enzymes database (CAZy) in 2013. *Nucleic Acids Res.* **42,** D490–D495 CrossRef Medline
15. Tardy, F., Nasser, W., Robert-Baudouy, J., and Hugouvieux-Cotte-Pattat, N. (1997) Comparative analysis of the five major *Erwinia chrysanthemi* pectate lyases: enzyme characteristics and potential inhibitors. *J. Bacteriol.* **179,** 2503–2511 CrossRef Medline
16. Kepseu, W. D., Sepulchre, J. A., Reverchon, S., and Nasser, W. (2010) Toward a quantitative modeling of the synthesis of the pectate lyases, essential virulence factors in *Dickeya dadantii*. *J. Biol. Chem.* **285,** 28565–28576 CrossRef Medline
17. Sepulchre, J. A., Mairet, F., and Gouzé, J.-L. (2017) Optimization and control of bio-conversion of polymeric substrate in the chemostat. *AIChE J.* **63,** 4738–4747 CrossRef
18. Kotoujansky, A., Lemattre, M., and Boistard, P. (1982) Utilization of a thermosensitive episome bearing transposon tn10 to isolate hfr donor strains of *Erwinia carotovora* subsp. *chrysanthemi*. *J. Bacteriol* **150,** 122–131 Medline
19. Miller, J. (1972) *Experiments in Molecular Genetics*, Cold Spring Harbor Laboratory, Cold Spring Harbor, NY
20. Moran, F., Nasuno, S., and Starr, M. P. (1968) Extracellular and intracellular polygalacturonic acid *trans*-eliminases of *Erwinia carotovora*. *Arch. Biochem. Biophys.* **123,** 298–306 CrossRef Medline
21. Nasser, W., Robert-Baudouy, J., and Reverchon, S. (1997) Antagonistic effect of crp and kdgr in the transcription control of the *Erwinia chrysanthemi* pectinolysis genes. *Mol. Microbiol.* **26,** 1071–1082 CrossRef Medline
22. Dochain, D. (ed) (2008) *Automatic Control of Bioprocesses*, Chapter 4, Wiley-ISTE, New York
23. Brühlmann, F. (1995) Purification and characterization of an extracellular pectate lyase from an *Amycolata* sp. *Appl. Environ. Microbiol.* **61,** 3580–3585 Medline
24. Nasser, W., Chalet, F., and Robert-Baudouy, J. (1990) Purification and characterization of extracellular pectate lyase from *Bacillus subtilis*. *Biochimie* **72,** 689–695 CrossRef Medline
25. Crawford, M. S., and Kolattukudy, P. (1987) Pectate lyase from *Fusarium solani* f. sp. pisi: purification, characterization, *in vitro* translation of the mRNA, and involvement in pathogenicity. *Arch. Biochem. Biophys.* **258,** 196–205 CrossRef Medline
26. Liao, C.-H., Sullivan, J., Grady, J., and Wong, L.-J. (1997) Biochemical characterization of pectate lyases produced by fluorescent pseudomonads associated with spoilage of fresh fruits and vegetables. *J. Appl. Microbiol.* **83,** 10–16 CrossRef
27. Bekri, M. A., Desair, J., Keijers, V., Proost, P., Searle-van Leeuwen, M., Vanderleyden, J., and Vande Broek, A. (1999) *Azospirillum irakense* produces a novel type of pectate lyase, *J. Bacteriol.* **181,** 2440–2447 Medline
28. Rao, M. N., Kembhavi, A. A., and Pant, A. (1996) Role of lysine, tryptophan and calcium in the β-elimination activity of a low-molecular-mass pectate lyase from *Fusarium moniliformae*. *Biochem. J.* **319**, 159–164 CrossRef Medline
29. Sawada, K., Ogawa, A., Ozawa, T., Sumitomo, N., Hatada, Y., Kobayashi, T., and Ito, S. (2000) Nucleotide and amino-acid sequences of a new-type pectate lyase from an alkaliphilic strain of bacillus. *Eur. J. Biochem.* **267,** 1510–1515 CrossRef Medline
30. Hatada, Y., Saito, K., Koike, K., Yoshimatsu, T., Ozawa, T., Kobayashi, T., and Ito, S. (2000) Deduced amino-acid sequence and possible catalytic residues of a novel pectate lyase from an alkaliphilic strain of bacillus. *Eur. J. Biochem.* **267,** 2268–2275 CrossRef Medline
31. Berensmeier, S., Singh, S. A., Meens, J., and Buchholz, K. (2004) Cloning of the pela gene from *Bacillus licheniformis* 14a and biochemical characterization of recombinant, thermostable, high-alkaline pectate lyase. *Appl. Microbiol. Biotechnol.* **64,** 560–567 CrossRef Medline